ELSEVIER

Physica C 367 (2002) 365–375

PHYSICA C

www.elsevier.com/locate/physc

Novel features of Josephson flux flow in Bi-2212: contribution of in-plane dissipation, coherent response to mm-wave radiation, size effect

Yu.I. Latyshev [a,b], A.E. Koshelev [c], V.N. Pavlenko [a,b,*], M.B. Gaifullin [d], T. Yamashita [a], Yuji Matsuda [d]

[a] *RIEC, Tohoku University, Katahira, Aoba-ku, Sendai 980-8577, Japan*
[b] *Institute of Radio-Engineering and Electronics, Russian Academy of Sciences, 11-7 Mokhovaya Str., Moscow 101999, Russia*
[c] *Materials Science Division, Argonne National Laboratory, Argonne, IL 60439, USA*
[d] *Institute for Solid State Physics, University of Tokyo, Kashiwanoha 5-1-5, Kashiwa, Chiba 277-8581, Japan*

Abstract

We studied Josephson flux flow (JFF) in Bi-2212 stacks fabricated from single crystal whiskers by focused ion beam technique. For long junctions with the in-plane sizes 30×2 μm^2, we found considerable contribution of the in-plane dissipation to the JFF resistivity, ρ_{Jff}, at low temperatures. According to recent theory [A. Koshelev, Phys. Rev. B 62 (2000) R3616] that results in quadratic type dependence of $\rho_{\mathrm{Jff}}(B)$ with the following saturation. The I–V characteristics in the JFF regime also can be described consistently by that theory. In the JFF regime we found Shapiro-step response to the external mm-wave radiation. The step position is proportional to the frequency of applied microwaves and corresponds to the Josephson emission from all the 60 intrinsic junctions of the stack being synchronized. That implies the coherence of the JFF over the whole thickness of the stack and demonstrates the possibility of synchronization of intrinsic junctions by the magnetic field. We also found a threshold character of the appearance of the JFF branch on the I–V characteristic with the increase of magnetic field, the threshold field B_{t} being scaled with the junction size perpendicular to the field L ($L = 30$–1.4 μm), as $B_{\mathrm{t}} \approx \Phi_0/Ls$, where s is the interlayer spacing. On the I–V characteristics of small stacks in the JFF regime we found Fiske-step features associated with resonance of Josephson radiation with the main resonance cavity mode in transmission line formed by stacks.

PACS: 74.72.Hs; 74.60.Ge
Keywords: Josephson flux flow; Josephson emission; Fiske steps

1. Introduction

Studies of interlayer tunnelling in layered high-T_{c} materials associated with intrinsic Josephson effects [1,2] lately became one of the most interesting issues developed in high-T_{c} superconductivity. Existence of the intrinsic Josephson effects and the related Josephson plasma oscillations are now quite well documented [3]. Of a particular

* Corresponding author. Address: Institute of Radio-Engineering and Electronics, Russian Academy of Sciences, 11-7 Mokhovaya Str., Moscow 101999, Russia. Tel.: +7-095-203-4976; fax: +7-095-203-8414.
E-mail address: vit@iname.com (V.N. Pavlenko).

0921-4534/02/$ - see front matter
PII: S0921-4534(01)01034-6

interest in this field is dynamics of Josephson vortex lattice (JVL) in long stacked junctions. JVL is formed in magnetic field parallel to the layers [4] and can be driven by dc current across the layers. Experimentally that was indicated as a resistive upturned flux-flow branch in the I–V characteristics with maximum voltage being proportional to magnetic field [5–7]. Maximum voltage corresponds to a condition, when the JVL velocity approaches the Swihart velocity [8], the velocity of electromagnetic wave propagation in the structure.

As it was pointed out recently [9] for highly anisotropic materials, as Bi-2212, the flux-flow resistivity at low temperatures can contain considerable contribution of the in-plane quasiparticle dissipation and thus can be used for extraction of the information about both quasiparticle conductivity components in superconducting state. This method still is not well elaborated. The coherent motion of JVL should induce coherent Josephson emission as it occurs in conventional long Josephson junctions [10]. The emission of that type can provide useful information about coherence of JVL motion. Therefore experiments on detection of Josephson emission in sliding JVL are very important. The interesting point in view of possible applications is also the short length limit for an observation of flux-flow regime. The present paper has been addressed to clarify the most of questions listed above. We have undertaken the detailed studies of the I–V characteristics and flux-flow resistivity in the sliding JVL regime. The data have been shown to be well consistent with recent theories of sliding JVL. We found Shapiro-step-type response of sliding JVL state to the external microwaves and Fiske-step features both pointing out to the existence of coherent Josephson emission in sliding JVL regime. The emission corresponds to the vertical synchronization of the major part or in some cases of all the number of elementary junctions in the stack. We also have studied flux-flow behavior with a decrease of the stack length down to $\sim$1 μm.

2. Experimental

The stacked structures have been fabricated by double-sided processing of high quality Bi-2212 whiskers [11] by focused ion beam. The stages of fabrications were similar to ones described in Ref. [12]. Fig. 1(a) shows schematically the geometry and orientation of the structure with respect to the crystallographic axes. The typical structure sizes L were $L_a = 1.5$–30 μm, $L_b = 1$–2 μm, $L_c = 0.05$–0.15 μm. The sizes and other parameters of the structures used in our studies are listed in Table 1. The oxygen doping level of the stacks estimated from $\rho_c(T)$ measurements above T_c [13] was nearly optimum, $\delta \approx 0.25$. The critical current density J_c at 4.2 K in the absence of magnetic field was 1–2 kA/cm^2 for the best samples.

Measurements of the I–V characteristics of Bi-2212 stacks have been carried out in commercial

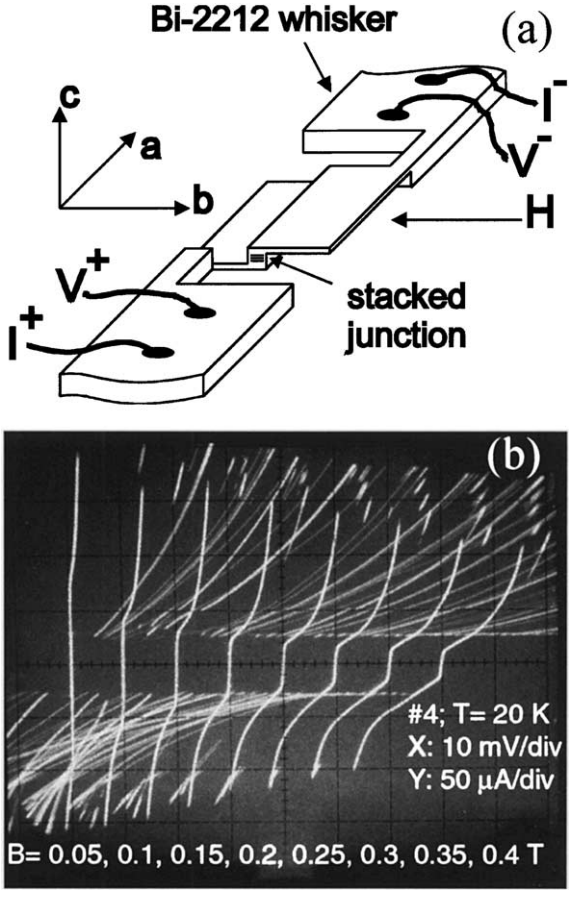

Fig. 1. Schematic view of the long Bi-2212 stack in experimental setup (a) and the I–V characteristics of junction #4 in magnetic field $B \| b$.

Table 1
Parameters of Bi-2212 stacked junctions

No.	L_a (μm)	L_b (μm)	N	I_c (μA)	Notes
4	28	2	90	550	
2	7	2	84	300	
7	3	2	81	140	
5	2	2	80	18	
H-1	1.5	1.5	90	0.6	Contains a hole $D = 0.2$ μm
H-3	1.5	1.5	80	0.3	Contains a hole $D = 0.2$ μm
6	30	2	57	1200	
8	28	2.5	75	1500	

cryostat of Quantum Design PPMS facility. The magnetic field has been oriented parallel to the b-axis within accuracy 0.1°. Field has been changed in steps of 0.1 T. In each fixed value of the field the back and forth I–V characteristics have been measured using fast oscilloscope. For the microwave measurements we used more advanced setup, the cryostat with slit pair superconducting magnet in the shielded room. The accuracy of magnetic field orientation $B\|b$ was 0.01°. External microwaves with a maximum incident power of 35 mW at the frequencies ranging from 45 to 142 GHz were applied from the backward-wave oscillators. The samples were mounted on the substrate that was placed at the center of the rectangular waveguides and was capacitively coupled with the flange of a waveguide. Thus the electrical component has been kept parallel to the c-axis.

3. Flux-flow resistivity and the I–V characteristics

Fig. 1(b) shows a set of the I–V characteristics of a long stack #4 at $T = 20$ K with subsequent increase of magnetic field B oriented parallel to the b-axis. The flux-flow branch and its evolution with magnetic field are clearly seen in the picture. The flux-flow branch appears just above I_c on the I–V characteristic. That is characterized by upturn and the maximum voltage, $V_{\rm Jff}$, above which the switch to the multibranched state occurs. As known [5–7] $V_{\rm Jff}$ linearly grows with field. We found the coefficient $dV_{\rm Jff}/dB$ to be 0.42 mV/T per elementary junction. Above approximately 1.7 T the slope of $V_{\rm Jff}(B)$ gradually increases to 0.86 mV/T (see also Ref. [6]). We define JFF resistance, $R_{\rm Jff}$, as initial linear part of the flux-flow branch. That can be find from linear extrapolation of the I–V to $V \to 0$. This extrapolation gives more reliable values for high fields above 0.3–0.5 T, when $I_c(B)$ becomes small. In the following two sections we consider the results of calculations of flux-flow resistivity dependence on magnetic field and the results of numerical calculations of flux-flow branch on the I–V characteristics, both based on the recent advanced approach [9,14,15] that takes into account the in-plane dissipation channel. Note that in earlier calculations [16–18] this contribution has been ignored. Comparison with experiment presented below proved the importance of the in-plane dissipation channel in JFF dynamics in Bi-2212.

3.1. Flux-flow resistivity

The linear flux-flow resistivity of the JVL, $\rho_{\rm Jff}$, is determined by the static lattice structure and linear quasiparticle dissipation. At high fields, $B > \Phi_0/\pi\gamma s^2$, Josephson vortices homogeneously fill all the layers and the static lattice structure is characterized by oscillating patterns of both c-axis and in-plane supercurrents. At small velocities this pattern slowly drifts along the direction of layers, preserving its static structure. This motion produces oscillating $\langle\tilde{E}_z\rangle$ and in-plane c-axis $\langle\tilde{E}_x\rangle$ electric fields leading to extra dissipation, in addition to usual dissipation due to the dc electric field E_z. Total dissipation per unit volume is given by

$$\sigma_{\rm Jff}E_z^2 = \sigma_c E_z^2 + \sigma_c\langle\tilde{E}_z^2\rangle + \sigma_{ab}\langle\tilde{E}_x^2\rangle, \quad (1)$$

where $\sigma_{\rm Jff} = 1/\rho_{\rm Jff}$ is the flux-flow conductivity, $\langle\cdots\rangle$ means time and space average, $\sigma_c = 1/\rho_c$ and $\sigma_{ab} = 1/\rho_{ab}$ are the c-axis and in-plane quasiparticle conductivities. An expansion with respect to Josephson current at high fields allows to derive a simple analytical formula for the flux-flow resistivity [9,14,15]:

$$\rho_{\rm Jff}(B) = \frac{B^2}{B^2 + B_\sigma^2}\rho_c, \qquad B_\sigma = \sqrt{\frac{\sigma_{ab}}{\sigma_c}}\frac{\Phi_0}{\sqrt{2}\pi\gamma^2 s^2}. \tag{2}$$

A relative importance of the in-plane and c-axis dissipation channels is determined by the dimensionless ratio $\sigma_{ab}/\sigma_c\gamma^2$. In high-$T_c$ superconductors at low temperatures, $T < 60$ K, this ratio is large $\sigma_{ab}/\sigma_c\gamma^2 = 20$–$50$, i.e., the in-plane channel dominates.

Eq. (2) describes very well the experimental field dependence of the flux-flow resistivity (Fig. 2). Fit of the experimental dependence $\rho_{\rm Jff}(T)$ by Eq. (2) at 4.2 K gives $\rho_c \approx 480\ \Omega$cm and $B_\sigma = 3.3$ T. This allows to extract the combination

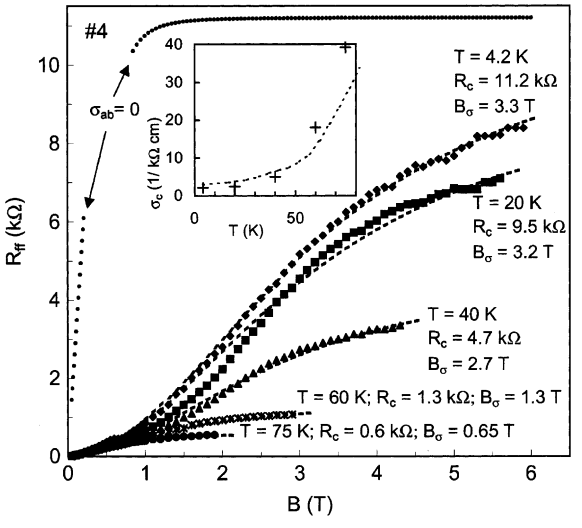

Fig. 2. Magnetic field dependence of the JFF resistance $R_{\rm Jff}$ for long Bi-2212 stack #4 at 4.2, 20, 40, 60, and 75 K. The dashed lines are fits to Eq. (2) for each temperature. The dotted curve is a calculated dependence $R_{\rm Jff}(B)$ at 4.2 K in a limit of zero in-plane dissipation ($\sigma_{ab} = 0$). The inset shows temperature dependence of σ_c: crosses obtained from the fit of $R_{\rm Jff}(B)$ to Eq. (2), the line corresponds to data obtained from measurements on small mesas in zero magnetic field [20].

$(\sigma_{ab}/\sigma_c\gamma^4)^{1/2} \approx 0.017$. Using for critical current density at low temperatures the value 1.7 kA/cm^2 we can estimate γ as $\gamma = 500$. That gives an estimate for $\sigma_{ab}(4.2\ {\rm K}) \approx 40\ (\mathrm{m\Omega\,cm})^{-1}$ which is quite close to the value $\sigma_{ab} \approx 60\ (\mathrm{m\Omega\,cm})^{-1}$ found at low temperatures from the microwave experiments [19].

Fig. 2 shows that experimental dependence $R_{\rm Jff}(B)$ is well described by the theory in wide temperature region 4.2–60 K. From the fit of experimental curves to Eq. (2) we can extract the temperature dependence of B_σ and σ_c (see insert to Fig. 2). As shown in insert, a dependence $\sigma_c(T)$ found in this way well agrees with dependence for $\sigma_c(T)$ extracted from the independent experiment on small mesas in zero magnetic field [20]. To extract the temperature dependence of σ_{ab} we need additional knowledge of the temperature dependence of γ. In principle that can be extracted from the temperature dependence of linear part of $R_{\rm Jff}(B)$ dependencies, but unfortunately the low field data of $R_{\rm Jff}(B)$ are not so reliable.

To demonstrate the importance of in-plane contribution in flux-flow resistivity we show in Fig. 2 two theoretical dependencies at 4.2 K, one is fitted to the experiment with finite σ_{ab} and another one is calculated with the same fitting parameters, but with zero in-plane dissipation contribution ($\sigma_{ab} = 0$). One can see huge inconsistency with experiment in the latter case.

3.2. Flux-flow branch

At high fields in the resistive state the interlayer phase differences grow approximately linearly in space and time

$$\theta_n(t,x) \approx \omega_E t + k_H x + \phi_n, \tag{3}$$

where ω_E is the Josephson frequency and k_H is magnetic wave vector. In the following we will use reduced parameters: $\omega \to \omega_E/\omega_{\rm p}$, $k_H \to k_H\gamma s$ (see Table 2). The most important degrees of freedom in this state are the phase shifts ϕ_n, which describe the structure of the moving JVL. In particular, for the static triangular lattice $\phi_n = \pi n$. Lattice structure experiences a nontrivial evolution with increase of velocity. The equations for ϕ_n can be derived from the coupled sine-Gordon equations for $\theta_n(t,x)$ by expansion with respect to the

Table 2
Meanings, definitions and practical formulas for the reduced parameters used throughout the paper

Notation	Meaning	Definition (CGS)	Practical formula (BSCCO)
ω_E	Reduced Josephson frequency	$\frac{2\pi csE_z}{\Phi_0\omega_p}$	$\frac{U\ [\mathrm{mV/junction}]}{2\times10^{-3}f_p\ [\mathrm{GHz}]}$
k_H	Magnetic wave vector	$\frac{2\pi H\gamma s^2}{\Phi_0}$	
v_c	c-Axis dissipation parameter	$\frac{4\pi\sigma_c}{\varepsilon_c\omega_p}$	$\frac{1.8\times10^3}{\varepsilon_c\rho_c\ [\Omega\mathrm{cm}]f_p\ [\mathrm{GHz}]}$
v_{ab}	In-plane dissipation parameter	$\frac{4\pi\sigma_{ab}\lambda_{ab}^2\omega_p}{c^2}$	$\frac{0.79(\lambda_{ab}\ [\mu\mathrm{m}])^2 f_p\ [\mathrm{GHz}]}{\rho_{ab}\ [\mu\Omega\mathrm{cm}]}$
l	Reduced London penetration depth	λ_{ab}/s	

In practical formulas $f=\omega_p/2\pi$ means plasma frequency, ρ_c and ρ_{ab} are the components of the quasiparticle resistivity.

Josephson current and averaging out fast degrees of freedom. In the case of steady state for a stack consisting of N junctions, this gives the following set of equations:

$$\frac{1}{2}\sum_{m=1}^{N}\mathrm{Im}[\mathsf{g}(n,m)\exp(\mathrm{i}(\phi_m-\phi_n))]=i_J, \tag{4}$$

where $i_J\equiv i_J(k_H,\omega_E)=\langle\sin\theta_n(t,x)\rangle$ is the reduced Josephson current, which has to be obtained as solution of these equations. The complex function $\mathsf{g}(n,m)$ describes phase oscillations in the mth layer excited by oscillating Josephson current in the nth layer. For a finite system it consists of the bulk term $G(n-m)$ and top and bottom reflections (multiple reflections can be neglected):

$$\mathsf{g}(n,m)=G(n-m)+\mathsf{B}G(n+m)+\mathsf{B}G(2N+2-n-m),$$

where

$$G(n)=\int\frac{\mathrm{d}q}{2\pi}\exp(\mathrm{i}qn)\left(\omega^2-\mathrm{i}v_c\omega-\frac{k^2(1+\mathrm{i}v_{ab}\omega)}{2(1-\cos q)+(1+\mathrm{i}v_{ab}\omega)/l^2}\right)^{-1}, \tag{5}$$

$\omega=\omega_E$ and $k=k_H$ are the frequency and the in-plane wave vector of the travelling electromagnetic wave generated by moving lattice. Dissipation parameters, v_c and v_{ab}, and reduced penetration depth l are defined in Table 2. $\mathsf{B}=\mathsf{B}(k,\omega)$ is the amplitude of reflected electromagnetic wave. For the practical case of the boundary between the static and moving Josephson lattices a detailed calculation of $\mathsf{B}(k,\omega)$ is presented in Ref. [15]. In general, quasiparticle conductivities in definitions of v_c and v_{ab} are the complex conductivities at the Josephson frequency. The frequency dependence is especially important for the in-plane conductivity. Recent terahertz spectroscopy measurements of $\sigma_{ab}(\omega)$ in BSCCO by Corson et al. [21] showed at low temperatures it has Drude frequency dependence with typical relaxation rate $1/\tau\approx1$ THz. Maximum Josephson frequency at the termination point of the flux-flow branch exceeds this value at fields $\geqslant 2$ T. Therefore the frequency dependence has to be taken into account. We use the Drude-like frequency dependence of $v_{ab}\equiv v_{ab}(\omega)$:

$$v_{ab}(\omega)=\frac{v_{ab0}}{1+\mathrm{i}\omega\tau}, \tag{6}$$

where τ is the quasiparticle relaxation time. Solution of Eq. (4) allows to obtain I–V characteristic as

$$j(E_z)=\sigma_cE_z+j_Ji_J(k_H,\omega_E),$$

where k_H and ω_E has to be expressed via magnetic and electric fields (see Table 2).

We solved Eq. (4) numerically and calculated the I–V dependencies for the first flux-flow branch. We used σ_c and σ_{ab}/γ^4 obtained from the fit of $\rho_{Jff}(B)$, assumed $\lambda_{ab}=200$ nm, and adjusted γ to

Table 3
Parameters of BSSCO used in calculation of the I–V dependencies

Penetration depth λ_{ab} (nm)	Anisotropy γ	Josephson current j_J (kA/cm^2)	In-plane conductivity σ_{ab} ([mΩcm]$^{-1}$)	c-Axis conductivity σ_c ([kΩcm]$^{-1}$)	Relaxation rate $1/\tau$ (THz)
200	500	1.7	39	2.1	$2\pi \times 0.55$

obtain the I–V dependencies most close to experimental ones. At high fields we found the fit can be significantly improved by taking into account frequency dependence of σ_{ab} via Eq. (6). Obtained parameters are summarized in Table 3. Typically, far away from the boundaries and the center, the solution has the form of a regular lattice, $\phi_{n+1} - \phi_n = \kappa$, where κ slowly decreases with ω_E starting from $\kappa = \pi$ at $\omega_E = 0$. Two lattice solutions, selected by the top and bottom boundaries, collide at the center forming defect region (shock). The first flux-flow branch terminates when $\kappa(\omega_E)$ intersects the instability boundary in the $\kappa - \omega_E$ plane. This corresponds to the maximum in the $j(E_z)$ dependence and happens when ω_E is somewhat smaller than the minimum frequency of the electromagnetic wave $\omega_{\min}(k)$ at fixed in-plane wave vector $k = k_H$. In reduced units $\omega_{\min}(k) = k/2$. For our parameters this corresponds to the voltage $V_{\min}(H)/H \approx 0.53$ mV/junction/T. Structure of the lattice at the instability point is shown in the insert to Fig. 3.

Again, as in previous section, we show for contrast a result of the I–V calculation with zero in-plane dissipation, $\sigma_{ab} = 0$ (the dashed curve in Fig. 3). One can see a high disagreement with experiment in that case. Theoretical curve is running far below the experimental and the resonance upturn near $V_{\max}$ is much sharper than in the experiment.

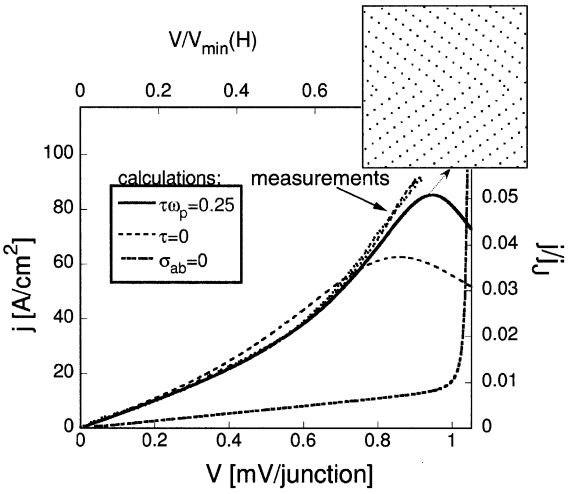

Fig. 3. Comparison of calculated and measured the I–V characteristic at $B = 2$ T. For calculation parameters see text. The inset shows vortex lattice structure near the $V = V_{\max}$.

4. Shapiro-step response of Josephson flux flow to external microwaves

As it was predicted theoretically [8] the coherent sliding of dense lattice of Josephson lattice in layered high-T_c materials should be accompanied by coherent microwave radiation with a frequency proportional to the lattice velocity. Alternatively, one can expect to find coherent DC response of Shapiro-step type on the I–V characteristics at the JFF regime under microwave radiation. Despite many studies of JFF regime in layered high-T_c materials [5–7], until recently there were practically no experiments on detection of coherent emission or Shapiro steps corresponding to sliding of JVL. Here we report on the observation of Shapiro-step-type response on flux-flow branch of the I–V characteristics of Bi-2212 "long" stacks under microwaves.

The I–V characteristics of samples #6 and #8 used for microwave experiments were typical to the Bi-2212 stacks with the multibranched structure [1] and critical current density $J_c = 1$–2 kA/cm^2 at 4.2 K. At fields $B > 0.03$ T we clearly observed flux-flow branch on the I–V characteristic. The properties of the flux-flow branch were similar to described in previous sections. We found that microwave irradiation induces Shapiro-step structure on the flux-flow branch. That is well resolved as a series of peaks on the derivative picture

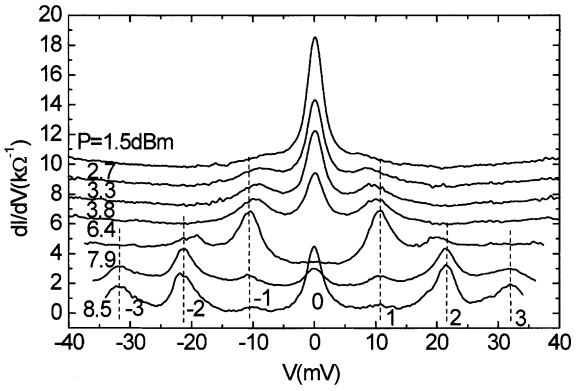

Fig. 4. The differential conductance of the stack #6 in flux-flow regime ($B = 2.4$ T, $B\|b$) as a function of microwave power of frequency 90.4 GHz, $T = 7.4$ K. Conductance scale corresponds to the lowest at 8.5 dBm, the other spectra are offset vertically.

$dI/dV(V)$ (Fig. 4). With an increase of microwave power P the voltage position of Shapiro steps V_{st}^{i}, does not depend on P and is only a function of microwave frequency f in accordance with the modified Josephson relation: $V_{st}^{i} = iNhf/2e$, with $i = p/q$; p, q are integers, N the number of the synchronized elementary junctions in the stack (Fig. 5). For one of two samples studied, #6, we found that N ($N = 57$) exactly corresponds to the whole number of the junctions in the stack ($N = 60 \pm 3$). As shown in Fig. 4 the amplitudes of both, Shapiro steps ΔI_c and critical current I_c are oscillatory functions of microwave power, the oscillations of the second step and I_c peaks being in-phase, whereas oscillations of the first step and I_c being in anti-phase. That resembles behavior of Shapiro steps and critical current for conventional tunnel Josephson junctions [22]. We found also that Shapiro steps are observed at fields B above 1 T corresponding to the conditions of dense lattice. However, the step position at fixed microwave frequency does not depend on B ($B = 1$–7 T) or temperature up to 75 K.

The presence of Shapiro steps on flux-flow branch of the I–V characteristics proves the existence of the coherent Josephson emission induced by sliding JVL. The Josephson-type relation between the voltage position of the step and external frequency points out to the in-plane coherency

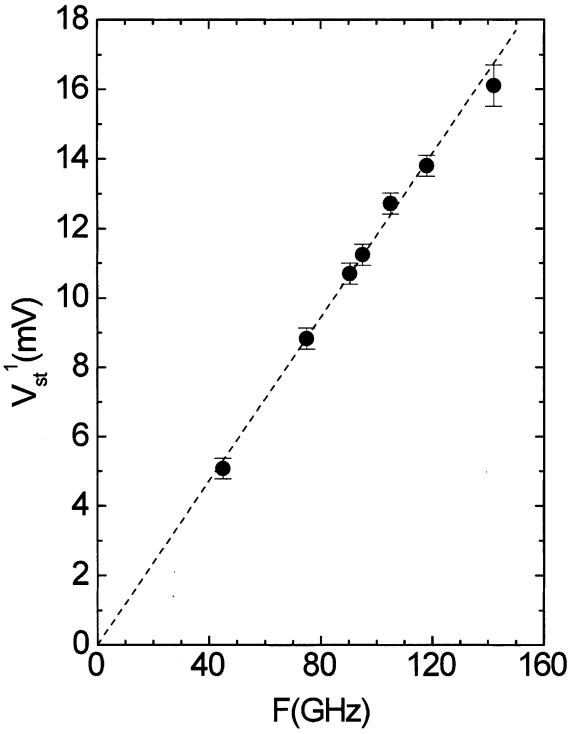

Fig. 5. Frequency dependence of the first Shapiro-step position, V_{st}^{1}, as a function of the frequency of microwave field for Bi-2212 stacked junction #6, $T = 7.4$ K, $B = 2.4$ T, $B\|b$. The straight line corresponds to the Josephson relation for $N = 57$.

of moving JVL, while the big coefficient N in Josephson relation proves the vertical coherence of the sliding JVL. Our results demonstrate the principal possibility of synchronization of elementary junctions by magnetic field. Because of the vertical synchronization of many junctions one can expect to get quite high power of the microwave emission. Our rough estimation of the emitted microwave power W at $f = 120$ GHz as $W \sim \Delta I_m V_{st}$ with ΔI_m the maximum step height gives the value $\sim 10^{-6}$ W.

5. Josephson flux-flow regime in short stacks

To investigate the JFF regime in a short length limit we fabricated a set of stacks of various lengths ranged from 30 down to 1.5 μm keeping the width of all the stacks the same, close to 2 μm.

We found that flux-flow regime can be achieved for all stacks including the smallest one but at different scale of magnetic field. The general feature found for the stacks of all length was the existence of threshold magnetic field B_t for the flux-flow regime. The flux-flow branch appears on the I–V characteristic only at fields exceeding B_t. B_t was found to increase with sample inverse length. For instance, for sample #4 with $L = 28$ μm B_t was 0.03 T while for the stack #7 with $L = 3$ μm B_t = 0.3 T. The log–log scale dependence of threshold field on the stack inverse length is shown in Fig. 6(a). That is very close to the linear dependence of $B_t(L^{-1})$ and practically does not depend on temperature at least at the interval 4.2–40 K. As it follows from Fig. 6(a) the found threshold field is close to the characteristic field B_0, $B_0 = \Phi_0/Ls$, corresponding to the condition of formation of the dense JVL (dashed line in Fig. 6(a). The threshold field B_t is found to scale with B_0 as $B_t = 0.63B_0$. The flux-flow branch for short samples was rather linear with slight upturn. The maximum voltage of flux-flow branch was generally less than for long stacks but asymptotically approached that for higher fields (Fig. 6(b)).

For stacks shorter than 5 μm we often observed sharp kinks on the flux-flow branch of the I–V characteristics (Fig. 7). The voltage position of the kink, V_k, is field independent and for #5 is equal to ≈15 mV. Sometimes we observed also second harmonic of the kink at double voltage $2V_k$. As shown in Fig. 7 the current amplitude of the kink ΔI_{k1} is oscillatory function of parallel magnetic field. The oscillations of $\Delta I_{k1}(B)$ are in anti-phase with the Fraunhofer oscillations of critical current (Fig. 8), while $\Delta I_{k2}(B)$ oscillates in phase with $I_c(B)$.

To discuss the threshold behavior of flux-flow we analyzed the value and size dependence of the first critical field B_{c1} for fluxon appearance in the stack. As it was pointed out in Ref. [23] B_{c1} increases with a decrease of sample size L as: $B_{c1} \approx (\Phi_0/L^2)(\lambda_c/\lambda_{ab})$. We plotted that dependence in Fig. 6(a) using the parameter: $\gamma = \lambda_c/\lambda_{ab} = 500$. The dependence $B_{c1}(L^{-1})$ is shown to lie below experimental points for $B_t(L^{-1})$. That means that at fields $B_{c1} < B < B_t$ the fluxons exist in the stack but do not contribute to the flux flow. We can

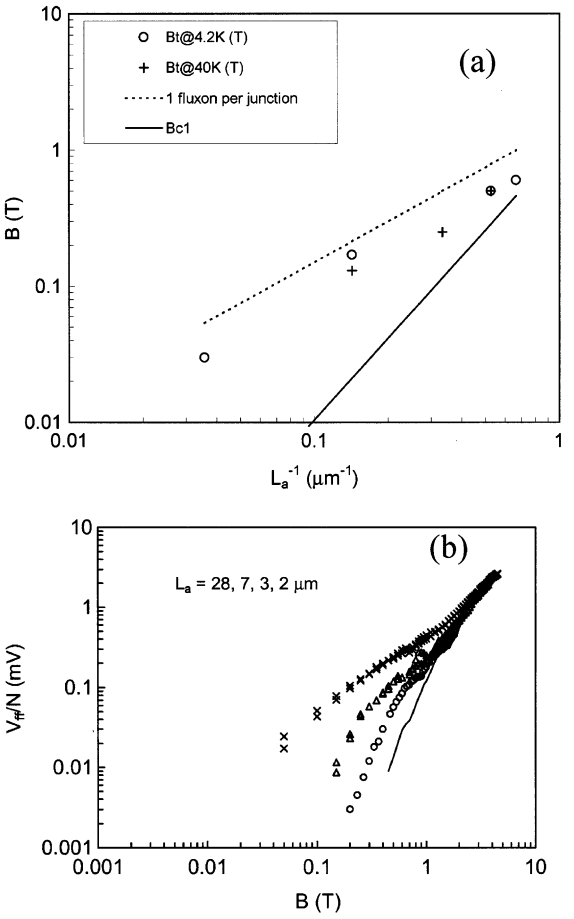

Fig. 6. (a) Experimental dependence of threshold magnetic field for appearance of the flux-flow branch on the I–V characteristics as a function of the inverse length of the stack. The dashed line corresponds to condition $B = \Phi_0/Ls$. Solid line corresponds to field B_{c1}: $B_{c1} = (\Phi_0/L^2)(\lambda_c/\lambda_{ab})$, (b) magnetic field dependence of maximum JFF voltage for stacks of different length.

consider that at those fields corresponding to dilute vortex lattice the pinning force is higher than the driving force up to the critical Josephson current across the layers. With field increase the lattice achieves dense limit and becomes rigid enough for collective motion. The increase of transverse rigidity leads to the effective reduction of pinning force, since the pinning force acting on individual fluxon will be effectively redistributed over the whole lattice. Thus we consider B_t as a threshold field when the driving force exceeds the pinning force acting on JVL. That turns out to be very near

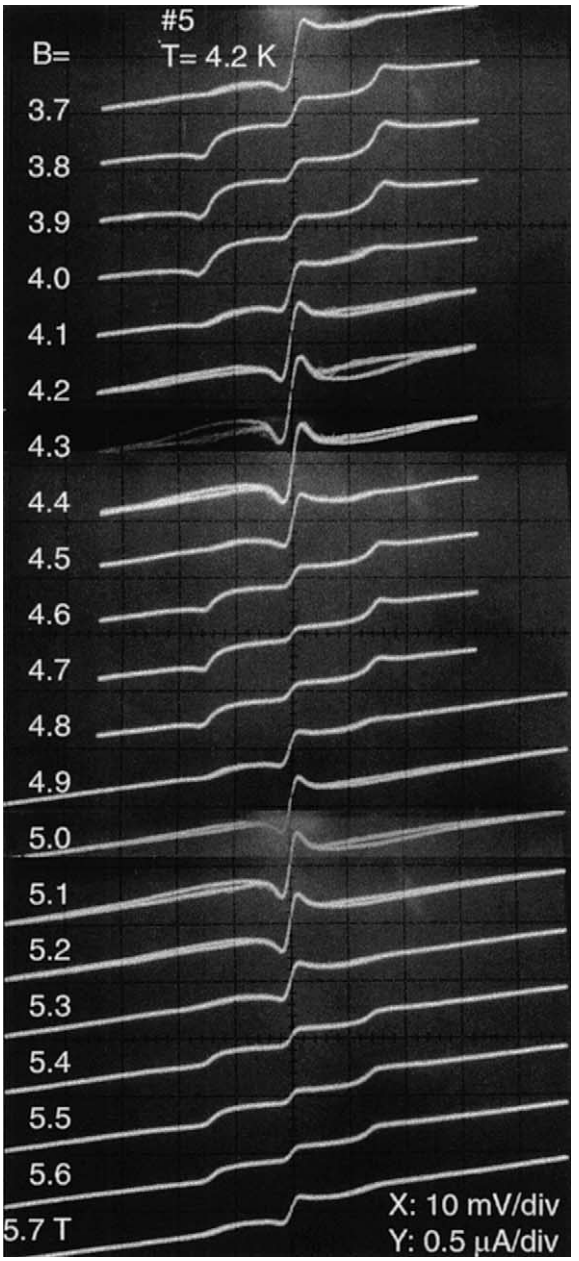

Fig. 7. A set of the I–V characteristics of a short Bi-2212 stack #5 with variation of parallel magnetic field $B_{\|}$ within 3.7–7.5 T, $T = 4.2$ K. Note a Fiske step at $V \approx 15$ mV.

to the condition of formation of dense lattice and corresponds to the transverse fluxon density 0.63 fluxon per junction.

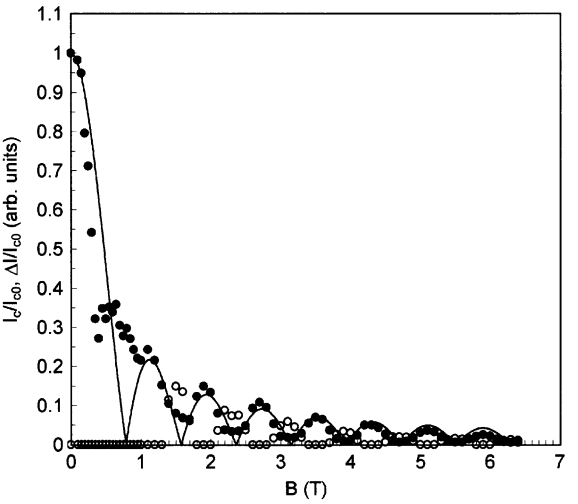

Fig. 8. (●)Magnetic field dependence of normalized critical current I_c/I_{c0} and (○) amplitude of the first Fiske step $\Delta I/I_{c0}$. $H\|b$, $T = 4.2$ K. Solid line is a fit to Fraunhofer dependence $I_c/I_{c0} = \sin x/x$ with $x = \pi BLs/\Phi_0$, $L = 2$ μm.

We can identify the kinks on the I–V characteristics of short stacks in JFF regime as the Fiske steps [24], which are known to appear due to the resonance of Josephson radiation with cavity modes in a transmission line formed by the junction. The characteristic features of the Fiske steps are as follows:

1. The step position follows the condition $V_m = mN\Phi_0 c_0/2L$ with m the integer, N the number of synchronized elementary junctions in the stack, c_0 the Swihart velocity, L the stack length.
2. Voltage position of the step is independent of B.
3. Current amplitude of the steps, ΔI_m, is periodic function of B with periodicity $\Delta B = \Phi_0/Ls$, even steps oscillating in-phase with I_c, while odd step oscillations being in anti-phase with $I_c(B)$ [25].

The conditions (2–3) are valid for our kink structure (see Figs. 7 and 8). The estimation of voltage position also gives reasonable value $V_{k1} =$ 14.2 mV. For estimation we used the following parameters $L = 2$ μm, $N = 80$, $\lambda_{ab} = 200$ nm, $s =$ 1.5 nm, $c_0/c = 1.19 \times 10^{-3}$. We estimated Swihart

velocity as the lowest mode valid for triangular lattice as [8] $c_0 = sc/2\lambda_{ab}(\varepsilon_c)^{1/2}$ with $\varepsilon_c = 10$. Note that the resonance frequency, $c_0/2L$, corresponding to the first Fiske step is quite high in our case $\approx$100 GHz. We observed Fiske steps on even shorter attacks with $L = 1.4$ μm.

The first indication of Fiske steps in Bi-2212 stacked junctions has been found in Refs. [26,27] on rather long junctions with $L = 20$–50 μm. The steps found [27] were unstable and not well reproducible. We consider that the better conditions of Fiske-step observation at short stacks are related with an increase of the resonance quality factor with decreasing L.

6. Conclusion

We carried out the detailed measurements of I–V characteristics in long Bi-2212 stacks in Josephson flux-flow regime and analyzed the data in the frame of recent theory taking into account both in-plane and out-of-plane channels for dissipation in JFF regime. We found that the experiment is well described by that theory. From the fit we found a number of Bi-2212 parameters at $T = 4.2$ K as σ_c, σ_{ab} and B_σ as well as the temperature dependence of σ_c, which agree well with those found by other methods. From that we can conclude that in-plane dissipation plays an important role in JFF regime at low temperatures.

By the experiments with external microwave radiation (45–142 GHz) we found a coherent Shapiro-step resonance on the I–V characteristic in JFF regime. That gives a strong evidence of the Josephson emission induced by coherently moving JVL.

For short stacks with length 1.5–2 μm we found the Fiske-step resonance which appears due to the resonance of Josephson radiation with cavity modes in transmission line formed by the stack. As in the case of Shapiro step response the Fiske-step position corresponds to the synchronization of all the 80 junction in the stack.

We also found that for stacks of different length the flux-flow branch appears above some threshold field $B_t = 0.63\Phi_0/Ls$.

Acknowledgements

We are thankful to A.M. Nikitina for providing us with Bi-2212 single crystal whiskers and S.-J. Kim for technical assistance. This work was supported by Japan Science and Technology Corp. and by Russian State Program on HTS (grant no. 99016).

References

[1] R. Kleiner, F. Steinmeyer, G. Kunkel, P. Mueller, Phys. Rev. Lett. 68 (1992) 2394;
R. Kleiner, P. Mueller, Phys. Rev. B 49 (1994) 1327.
[2] As a resent review see A.A. Yurgens, Supercond. Sci. Technol. 13 (2000) R85.
[3] See Proceedings of the 1st and 2nd International Symposium on Intrinsic Josephson Effects and THz Plasma Oscillations in High Temperature Superconductors, Physica C 293 (1997); Physica C 362 (2001).
[4] L.N. Bulaevskii, J. Clem, Phys. Rev. B 44 (1991) 10234.
[5] J.U. Lee, J.E. Nordman, G. Hoherwarter, Appl. Phys. Lett. 67 (1995) 1471;
J.U. Lee, P. Guptasarma, D. Hornbaker, A. El-Kortas, D. Hinks, K.E. Gray, Appl. Phys. Lett. 71 (1997) 1412.
[6] G. Hechtfischer, R. Kleiner, A.V. Ustinov, P. Mueller, Phys. Rev. Lett. 79 (1997) 1365;
G. Hechtfischer, R. Kleiner, K. Schlenga, W. Walkenhorst, P. Mueller, H.L. Johnson, Phys. Rev. B 55 (1997) 14638.
[7] Yu.I. Latyshev, P. Monceau, V.N. Pavlenko, Physica C 282–287 (1997) 387;
Yu.I. Latyshev, P. Monceau, V.N. Pavlenko, Physica C 293 (1997) 174.
[8] L.N. Bulaevskii, D. Domingez, M.P. Maley, A.R. Bishop, B.I. Ivlev, Phys. Rev. B 53 (1996) 14601.
[9] A.E. Koshelev, Phys. Rev. B 62 (2000) R3616.
[10] T. Nagatsuma, K. Enpuku, F. Irie, K. Yoshida, J. Appl. Phys. 54 (1983) 3302.
[11] Yu.I. Latyshev, I.G. Gorlova, A.M. Nikitina, V.U. Antokhina, S.G. Zybtsev, N.P. Kukhta, V.N. Timofeev, Physica C 216 (1993) 471.
[12] Yu.I. Latyshev, S.-J. Kim, T. Yamashita, IEEE Trans. Appl. Supercond. 9 (1999) 4312.
[13] T. Watanabe, T. Fujii, A. Matsuda, Phys. Rev. Lett. 79 (1997) 2113.
[14] A.E. Koshelev, I.S. Aranson, Phys. Rev. Lett. 85 (2000) 3938.
[15] A.E. Koshelev, I.S. Aranson, cond-mat/0104374.
[16] J.R. Clem, M.W. Coffey, Phys. Rev. B 42 (1990) 6209.
[17] S. Sakai, A.V. Ustinov, H. Kohlstedt, A. Petraglia, N.F. Pedersen, Phys. Rev. B 50 (1994) 12905.
[18] M. Machida, T. Koyama, A. Tanaka, M. Tachiki, Physica C 330 (2000) 85.

[19] S.-F. Lee, D.C. Morgan, R.J. Ormeno, D.M. Broun, R.A. Doyle, J.R. Waldram, K. Kadowaki, Phys. Rev. Lett. 77 (1996) 735;
H. Kitano, T. Hanaguri, Y. Tsuchiya, K. Iwaya, R. Abiru, A. Maeda, J. Low Temp. Phys. 117 (1999) 1241.
[20] Yu.I. Latyshev, T. Yamashita, L.N. Bulaevskii, M.J. Graf, A.V. Balatsky, M.P. Maley, Phys. Rev. Lett. 82 (1999) 5345.
[21] J. Corson, J. Orenstein, S. Oh, J. O'Donnell, J.N. Eckstein, Phys. Rev. Lett. 85 (2000) 2569.
[22] A. Barone, G. Paterno, Physics and Applications of the Josephson Effect, Wiley, New York, 1982.
[23] Yu.I. Latyshev, J.E. Nevelskaya, P. Monceau, Phys. Rev. Lett. 77 (1996) 932.
[24] M.D. Fiske, Rev. Mod. Phys. 36 (1964) 221.
[25] I.O. Kulik, JETP Lett. 2 (1965) 84.
[26] A. Irie, Y. Hirai, G. Oya, Appl. Phys. Lett. 72 (1998) 2159.
[27] V.M. Krasnov, N. Mros, A. Yurgens, D. Winker, Phys. Rev. B 59 (1999) 8463.